Electronic Supplementary Information

A Multi-cation Responsive Ni(II)-Supramolecular Metallogel Mimics as Molecular Keypad Lock *via* Reversible Fluorescence Switching

Vaishali Singh[a], Shubhra Kala[b], Tanmay Rom[c], Avijit Kumar Paul[c] and Rampal Pandey*[a]

[a]National Institute of Technology Uttarakhand, Srinagar (Garhwal)-246174, INDIA.
[b]Hemwati Nandan Bahuguna Garhwal University, Srinagar (Garhwal)-246174, INDIA.
[c]National Institute of Technology Kurukshetra, Kurukshetra -136119, INDIA.

Preparation of [Zn($C_{21}H_{29}N_3O_2$)] (2). Complex **2** was prepared following above synthetic procedure adopted for **1** to obtain orange precipitate. The grown single crystals immediately lose their transparency and become inappropriate for diffraction. Yield (1.1 g; 59.3%) Anal Calcd. [$C_{42}H_{56}N_6ZnO_2$]: C 67.96; H 7.60; N 11.32 %; Found: C 67.76; H 7.67; N 11.24 %; FT-IR (cm^{-1}): 2968, 1610, 1567, 1490, 1346, 1203, 1132, 823, 778. ^{1}H-NMR ($CDCl_3$, 400 MHz, δ_H, ppm): 8.47 (s, 2H, -C*H*=N-), 7.57-7.47 (s, 2*H*, Ar), 7.42-7.21 (d, 4*H*, Ar), 6.92-6.71(d, 4*H*, Ar), 6.47-6.40(d, 2*H*, Ar) 6.32(d, 2*H*, Ar), 3.39-3.35 (m, 16*H*, -CH_2), 1.97-1.24 (m, 24*H*, -CH_3) ^{13}C NMR ($CDCl_3$, 125 MHz, δ_C, ppm): 161.82, 160.47, 147.97, 136.16, 80.52, 72.11, 69.76, 69.52. ESI-MS (m/z) for $C_{42}H_{56}N_6ZnO_2$: Calcd. [M^+] 740.3756; found [M+H]$^+$: 741.3806.

Spectral analysis of complex 2. ^{1}H NMR spectrum of complex **2** displayed complete vanishing of phenolic -OH peak of **HL** along with significant down-field shifts in the -C*H*=N- ($\Delta\delta$, 0.07 ppm. Other aromatic and aliphatic resonances were also deshielded in **2** relative to that of **HL** (Fig. S2, ESI†). The Electrospray ionization-mass spectrometry (ESI-MS) also strongly suggested the formation of metal complex **2** by exhibiting abundant molecular ion peaks [M+H]$^+$ at 741.3806 (Fig. S3, ESI†) thereby supporting the 2:1 (**L**$^-$: **M**) stoichiometric complexation between ligand and metal ion. Furthermore, formation of complex **2** was elucidated with the help of FT-IR spectral analysis in the solid-state. Several symmetric and asymmetric vibrations appeared in the FT-IR spectra for **2**. The FT-IR spectrum for **HL** shows vibration at 1615 cm^{-1} that may be ascribed to the azomethine (>C=N-) stretching[23] which is considerably shifted toward low frequency region in the complex **2** to appear at 1608 cm^{-1} (Fig. S4, ESI†).

Table S1 Crystal data and refinement structural parameters of **HL** and **1**.

Structural parameter	**HL**	**Complex (1)**
Empirical formula	$C_{21}H_{29}N_3O$	$C_{42}H_{56}N_6O_2Ni$
Formula weight	339.47	735.63
T(K)	295	296
λ (Mo Kα) (Å)	0.71073	0.71073
Crystal system	Orthorhombic	Triclinic
Space group	*P*212121	*P*-1 (No. 2)
a (Å)	8.1986(4)	9.0649(4)
b (Å)	9.7128(4)	9.0718(4)
c (Å)	24.4172(12)	12.9046(6)
α (deg.)		72.800(1)
β (deg.)		75.386(1)
γ (deg.)		73.838(2)
V (Å)	1944.38(16)	956.83(8)
Z	4	1
D (g cm^{-3})	1.160	1.277
μ (min^{-1})	0.07	0.551
F (000)	736	394
θ range (deg.)	2.3 to 25.4	1.681to 25.000
Reflections collected	29,557	3319
Unique data	3556	3027
R indexes [$I > 2\ \sigma(I)$]		$R_1 = 0.0306$ $wR_2 = 0.0801$
R indexes (all data)	$R_1 = 0.064$ $wR_2 = 0.205$	$R_1 = 0.0372$ $wR_2 = 0.0909$
GOF on F^2	1.07	1.126
$\sum \lVert F_O \rvert - \lvert F_C \rVert / \sum \lvert F_O \rvert$. $wR_2 = \{\sum [w (F_O^2 - F_C^2)]/\sum [w (F_O^2)^2]\}^{1/2}$. Empirical formula and formula weight of all the compounds are given from CIF files.		

Table S2 Selected bond distances (Å) and angles (°) marked in **1**.

Bond	**Length (Å)**
Ni(1)—O(1)	1.838(1)
Ni(1)—N(2)	1.913(1)
C(2)—N(1)	1.453(2)
C(3)—N(1)	1.450(3)
C(5)—N(1)	1.383(2)
C(8)—N(2)	1.441(2)
C(11)—N(2)	1.294(2)
C(15)—N(3)	1.376(2)
C(19)—N(3)	1.460(3)
C(20)—N(3)	1.454(3)
Bond	**Angle (deg.)**

O(1)—Ni(1)—O(1)	180.00(6)
O(1)—Ni(1)—N(2)	87.16(5)
C(3)—N(1)—C(2)	117.57(1)
C(5)—N(1)—C(2)	120.80(1)
C(5)—N(1)—C(3)	121.05(1)
C(11)—N(2)—C(8)	116.04(1)
C(15)—N(3)—C(19)	121.73(1)
C(15)—N(3)—C(20)	121.03(1)
C(20)—N(3)—C(19)	117.12(1)

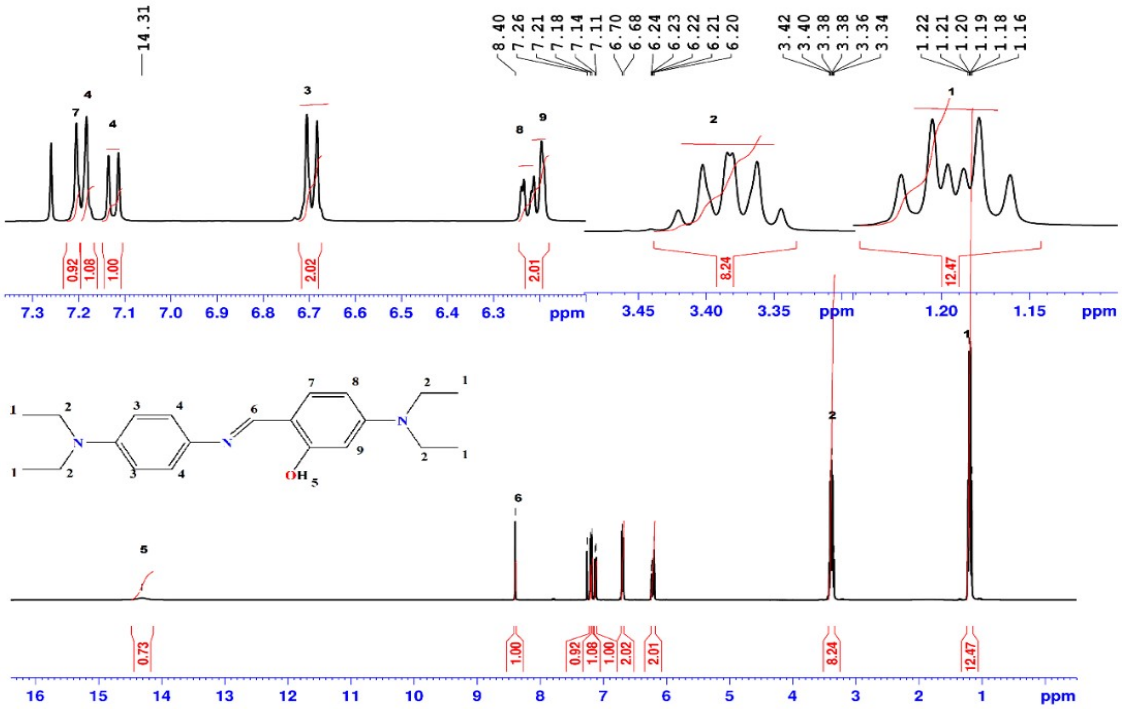

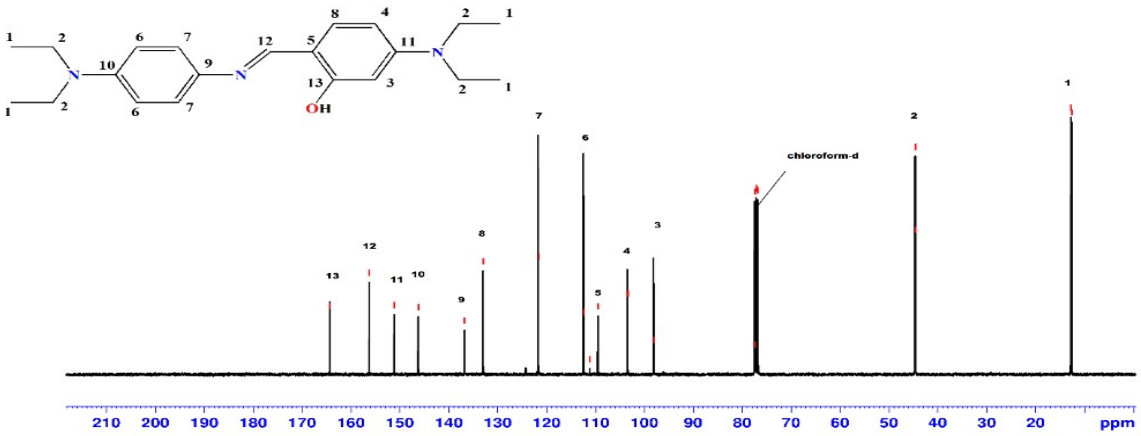

Fig. S1 ^{1}H-NMR and ^{13}C-NMR Spectra of **HL**.

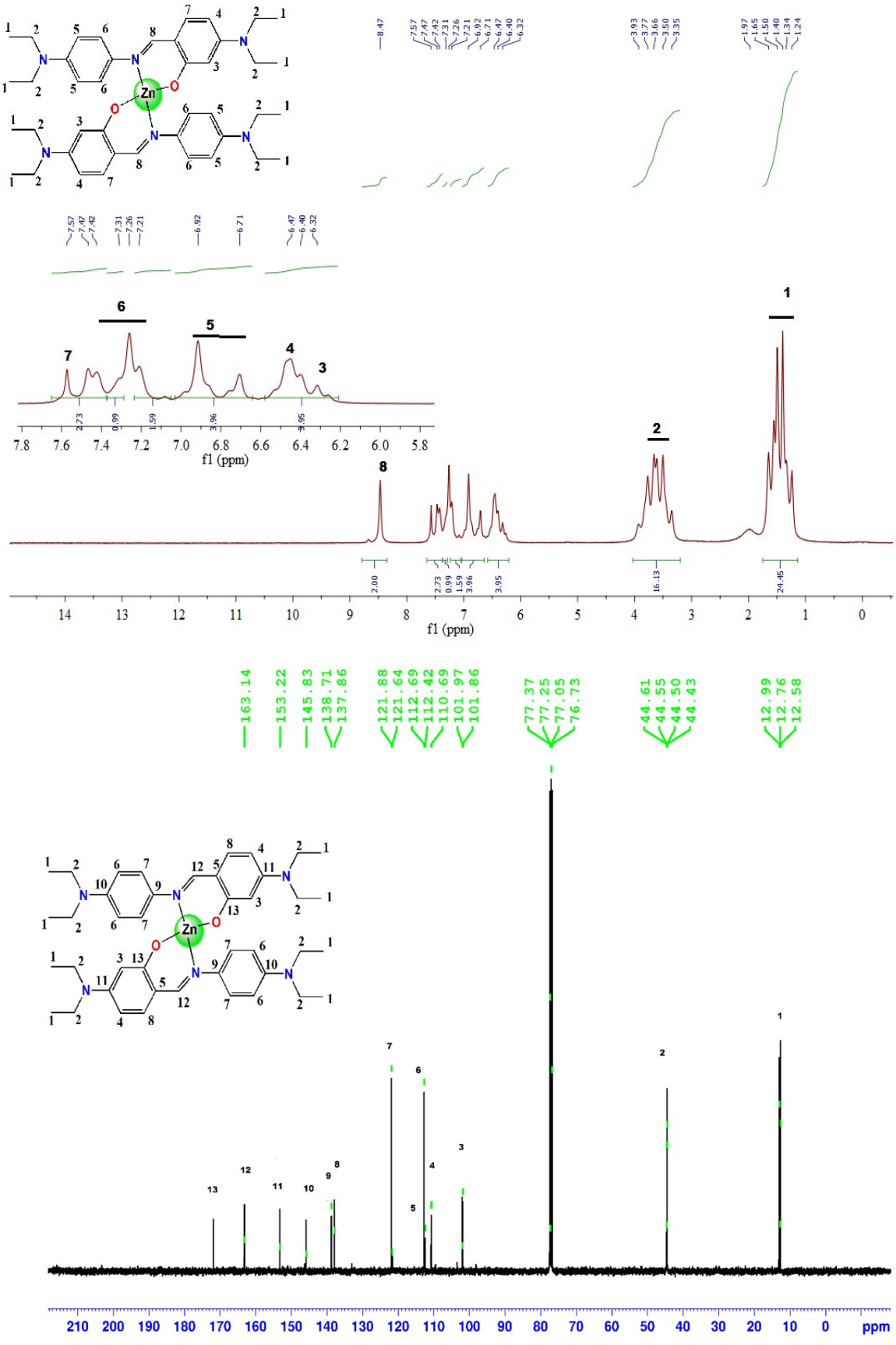

Fig. S2 ^{1}H-NMR and ^{13}C-NMR spectra of **2.**

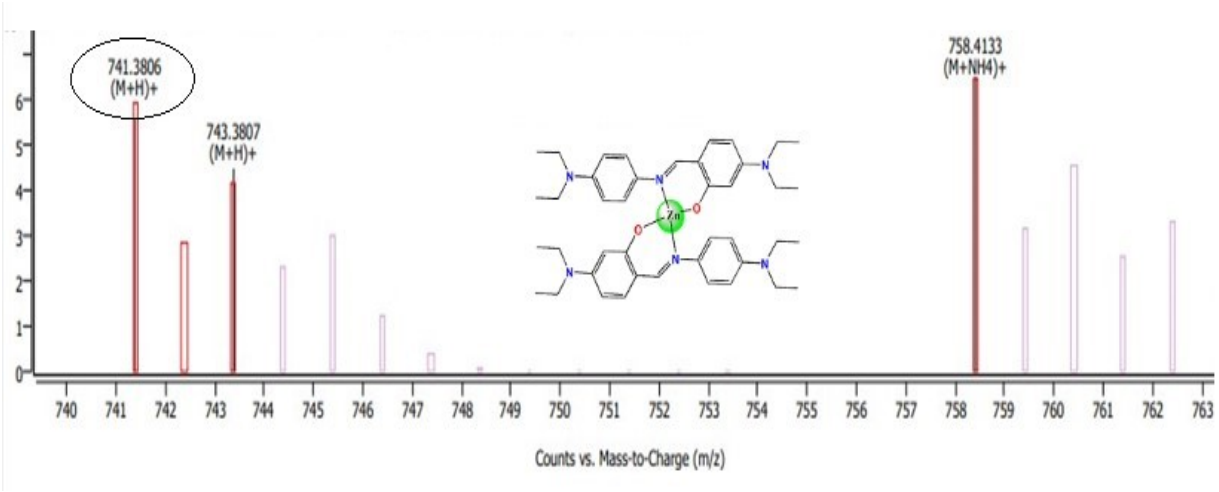

Fig. S3 ESI-MS spectrum of **2**.

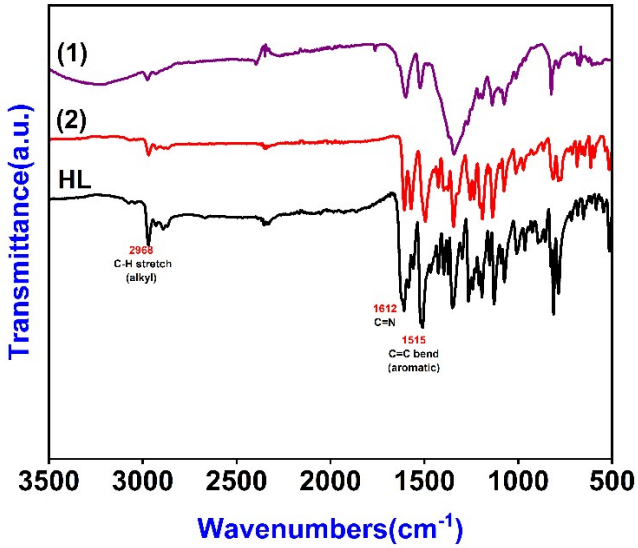

Fig. S4 FT-IR spectra of **HL** and **1-2**.

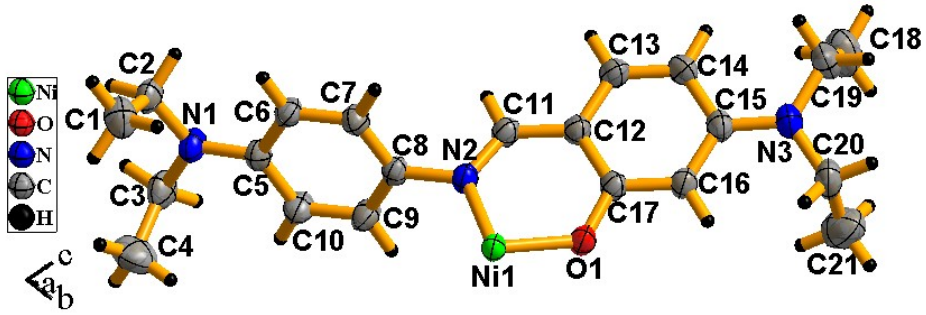

Fig. S5 The asymmetric unit of **1** with 50% probability displacement ellipsoid.

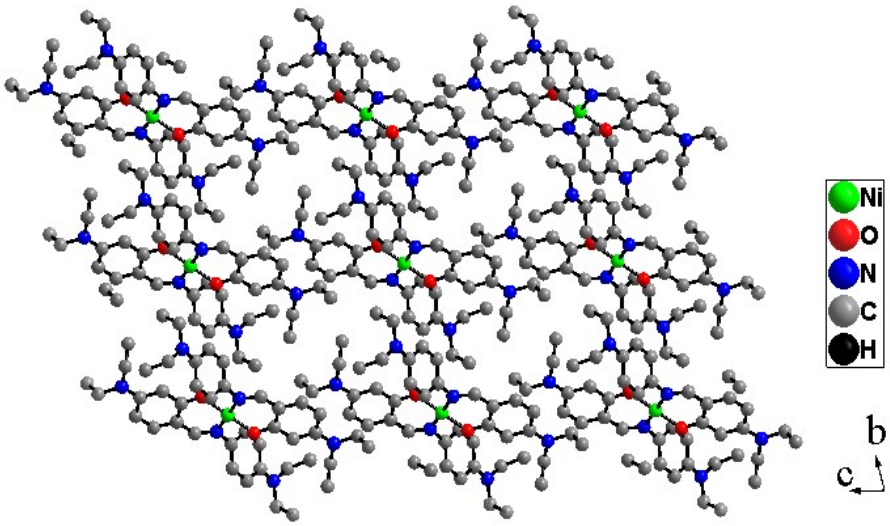

Fig. S6 The overall packing structure of **1** in *bc* plane.

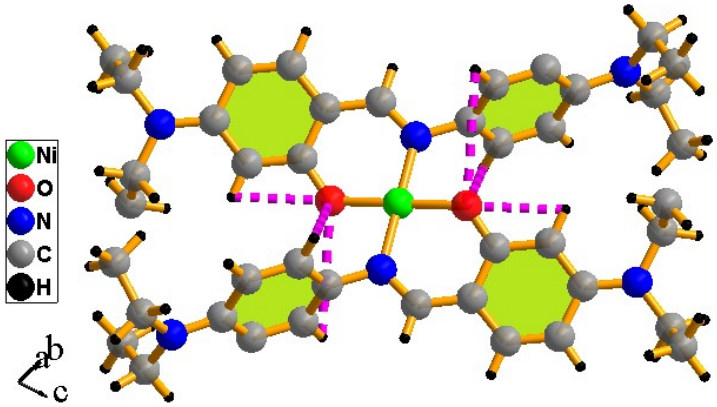

Fig. S7 The observed intra-molecular hydrogen bonding interaction in structure of **1.**

S.No.	Solvent	Solubility
1	Methanol	Slightly soluble
2	Ethanol	Slightly soluble
3	Acetonitrile	Partially soluble
4	Dimethyl sulfoxide	Partially soluble
5	**Dimethyl formamide**	**Soluble**
6	**Acetone**	**Soluble**
7	**Dichloromethane**	**Soluble**
8	**Chloroform**	**Soluble**
9	**Tetrahydrofuran**	**Soluble**
10	Diethyl ether	Insoluble
11	Hexane	Insoluble

Table S3 Solubility of **HL**.

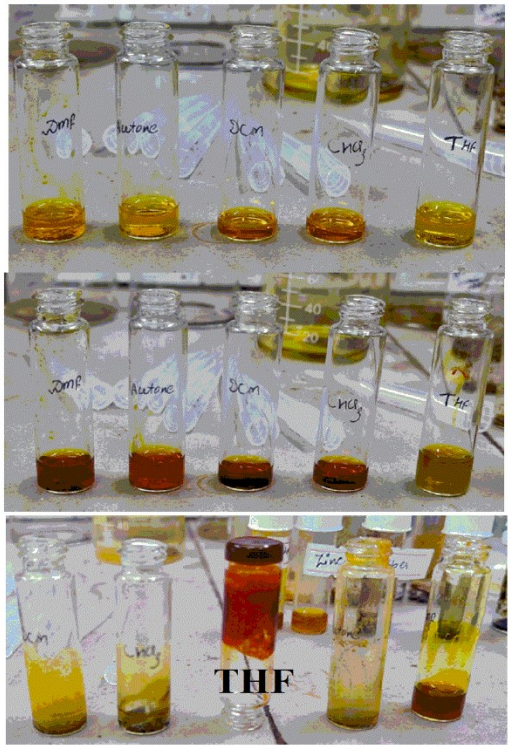

Fig. S8 Photograph of instantaneous gel material in the presence of THF solvent.

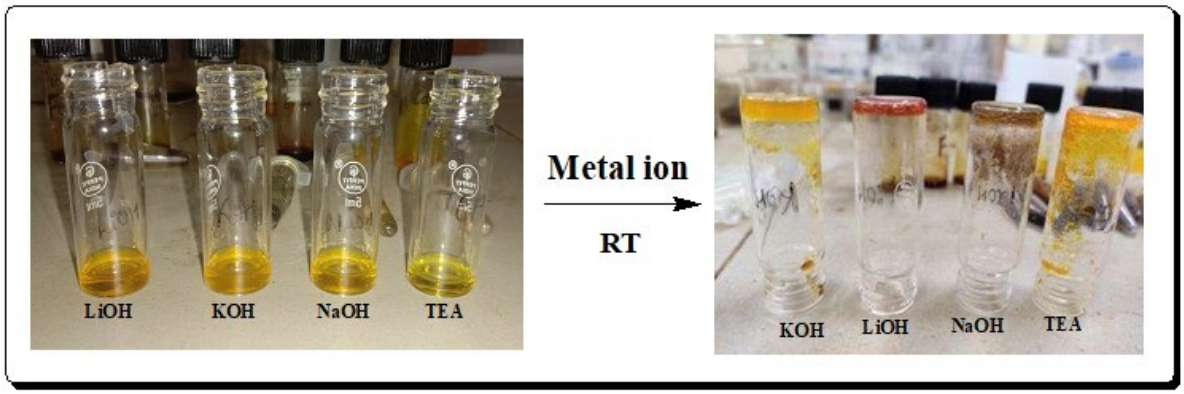

Fig. S9 Photograph of instantaneous gel material with different base (MeOH).

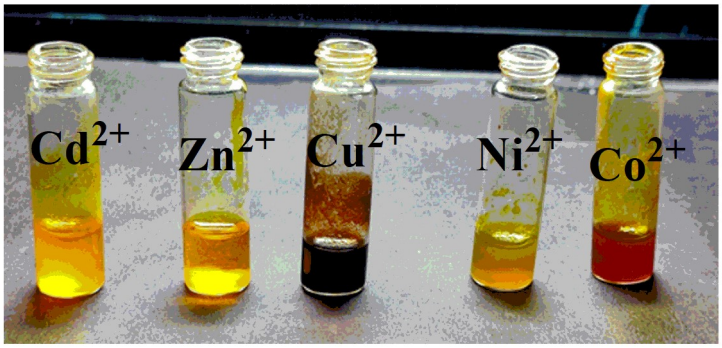

Fig. S10 To know the ability of gelation with a stoichiometry (2:1) of **HL** with Ni^{2+}metal ion.

S.No.	Ligand (0.1 mmol in THF)	Base (0.2 mmol TEA)	Metal nitrates (0.1 mmol in MeOH)	Instant Observation
1	1mL	32µL	Cd^{2+}=30 mg	PG
2	1mL	32µL	Zn^{2+}=32 mg	P
3	1mL	32µL	Cu^{2+}=23 mg	P
4	1mL	32µL	Ni^{2+}=30 mg	G
5	1mL	32µL	Co^{2+}=30 mg	P

S=Solution, P=Precipitate, PG=Partially Gel, G=Gel

Table S4 The tabulated represents the gelation ability of the **HL** with stoichiometry (1:1).

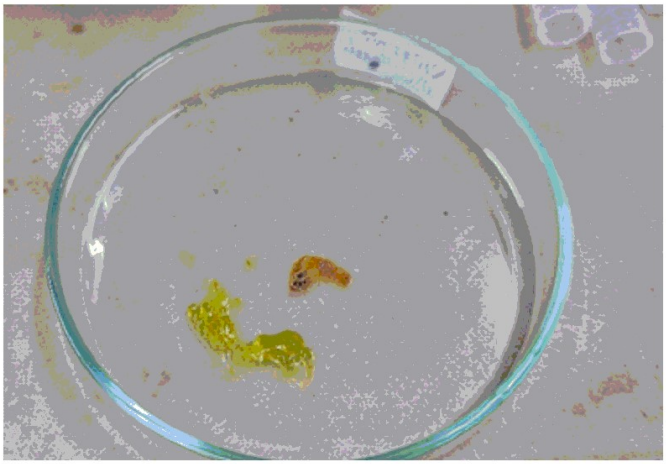

Fig. S11 Image of xerogel **MG** on increasing temperature upto 50°C with compared freshly **MG**.

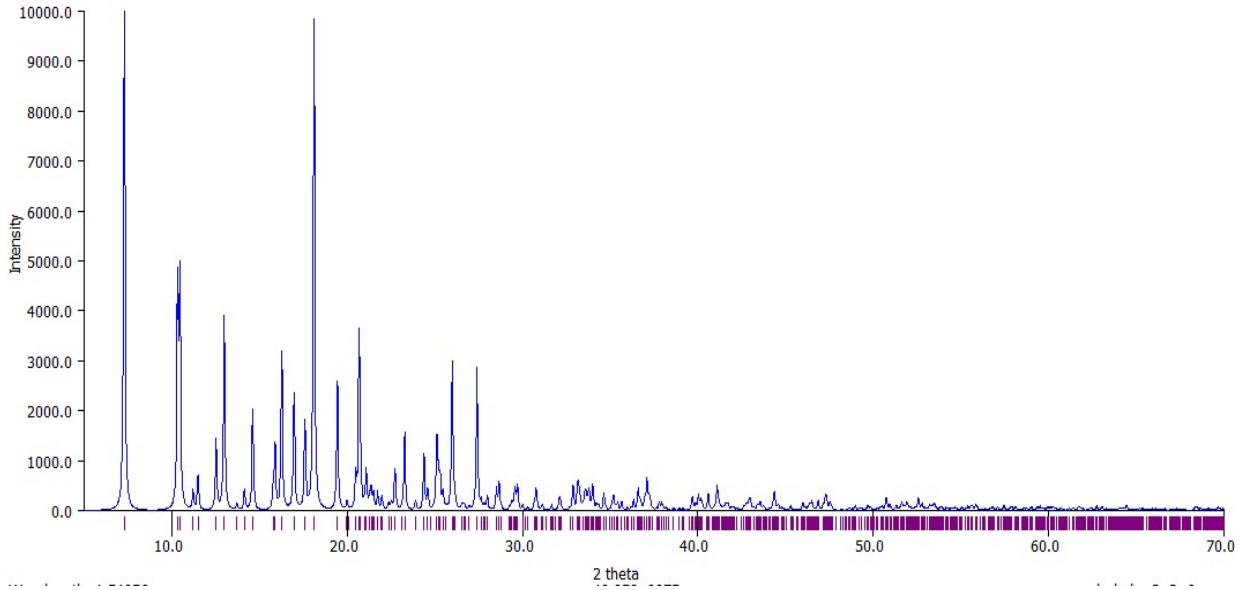

Fig. S12 PXRD pattern of the complex **1**.

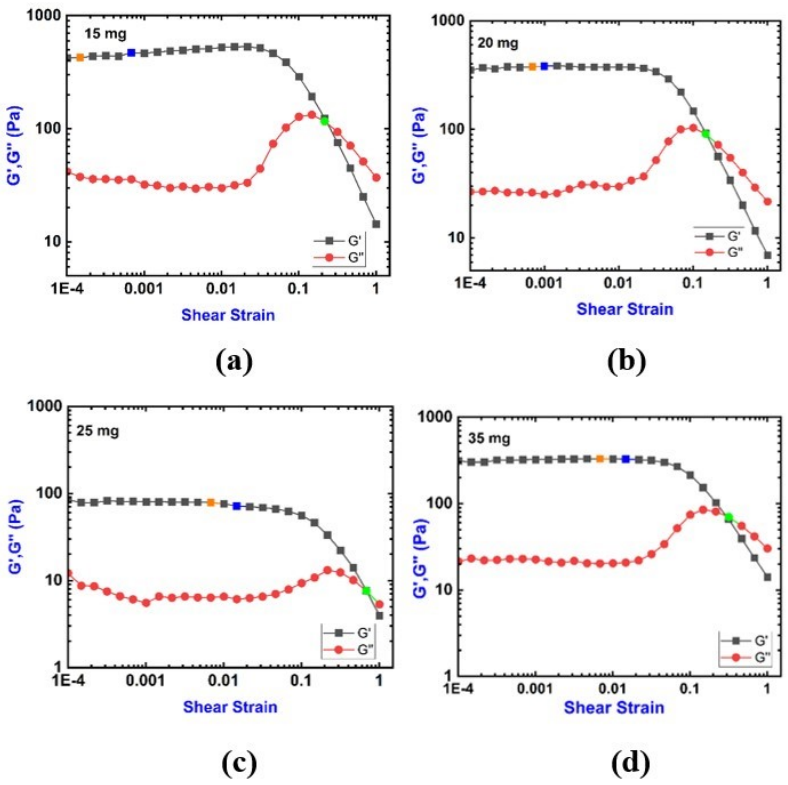

Fig. S13 Amplitude sweeps measurements of **MG** with shear strain 0.01% at different concentration of Ni^{2+} ion (a)15 mg (b) 20 mg (c) 25 mg (d) 35 mg.

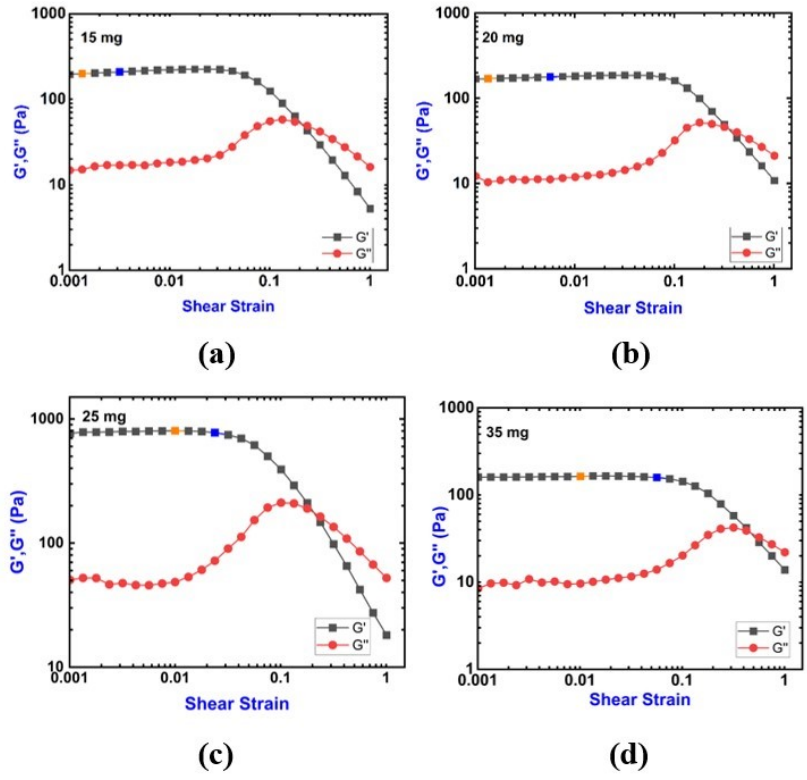

Fig. S14 Amplitude sweeps measurements of **MG** with shear strain 0.1% at different concentration of Ni^{2+} ion (a) 15 mg (b) 20 mg (c) 25 mg (d) 35 mg.

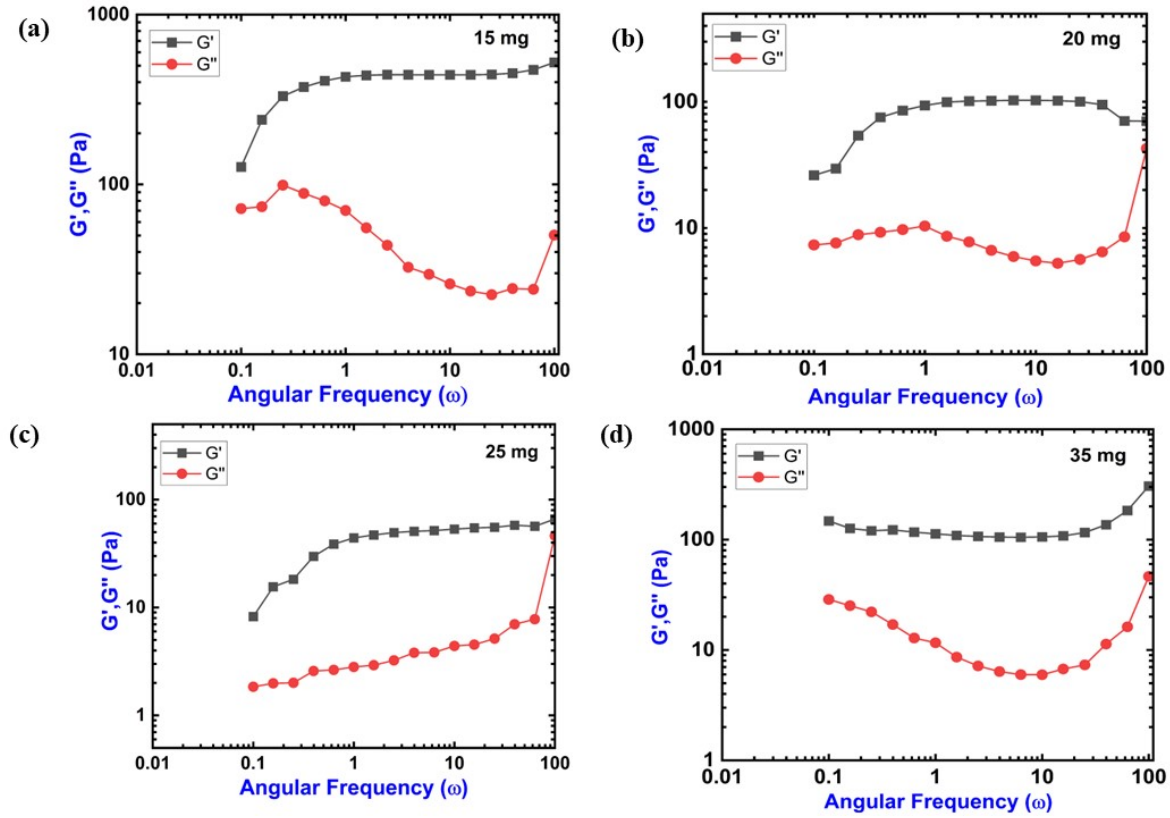

Fig. S15 Frequency sweeps measurements of **MG** with constant strain 0.5% at different concentration of Ni^{2+} ion (a) 15 mg (b) 20 mg (c) 25 mg (d) 35 mg.

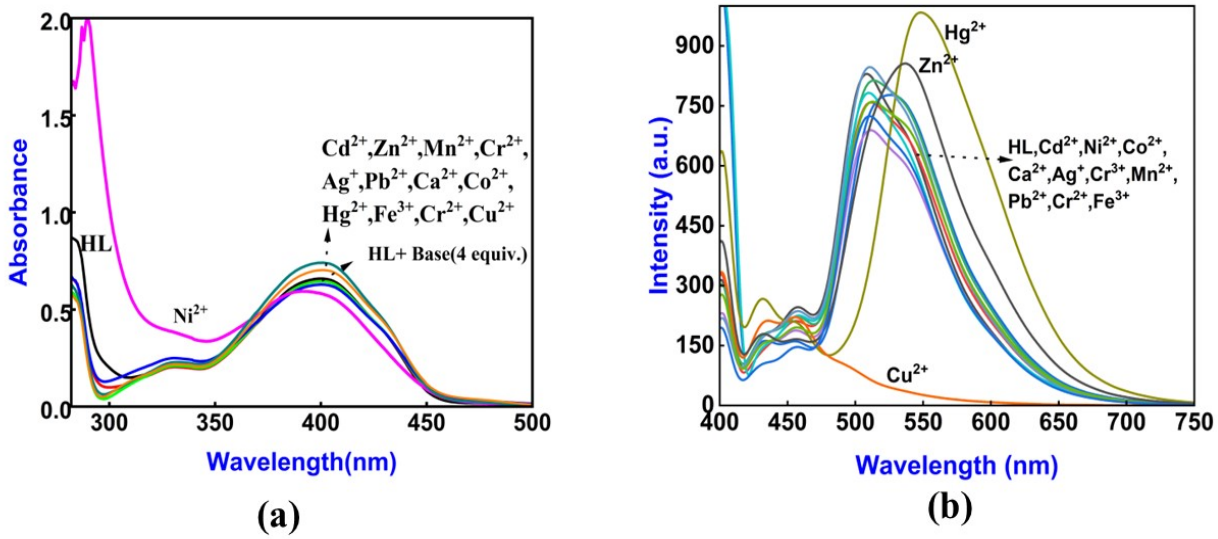

Fig. S16 (a) Absorption spectra in presence of TEA base (100mM, MeOH) with metal nitrates (100 mM, MeOH) and (b) Emission spectra of **HL**(10 μM, THF) absence of base with metal nitrates (100 mM, MeOH).

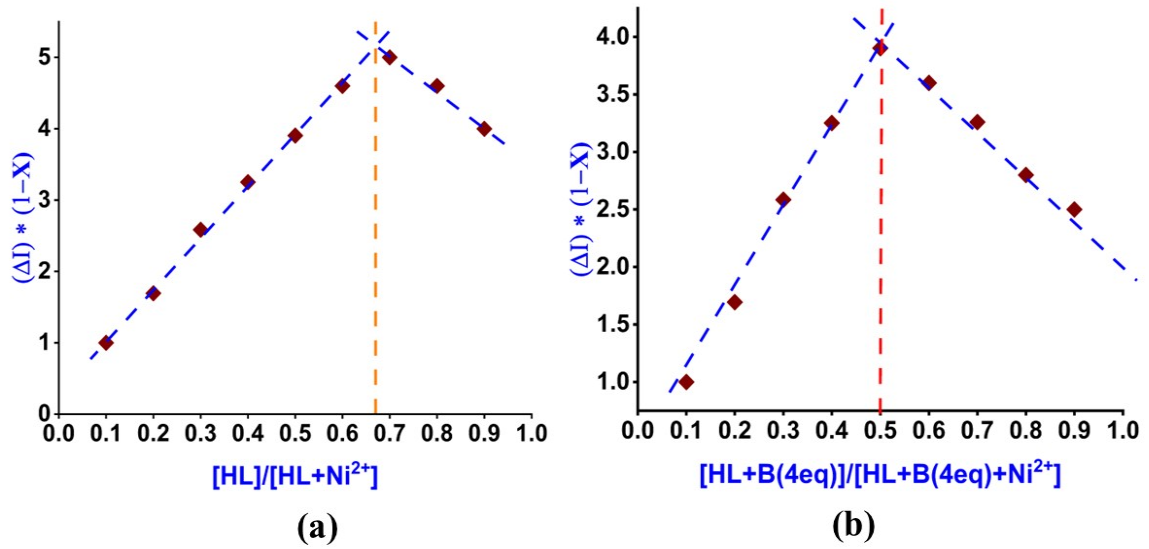

Fig. S17 (a)Job's plot analysis showing 2:1 stoichiometry between **HL** (10 µM, THF) and Ni^{2+} ion (10 µM, MeOH) without base (b) Job's plot analysis showing 1:1 stoichiometric between **HL** (10 µM, THF) and Ni^{2+} metal ion (10 µM, MeOH) with TEA (4equiv., 10 µM, MeOH).

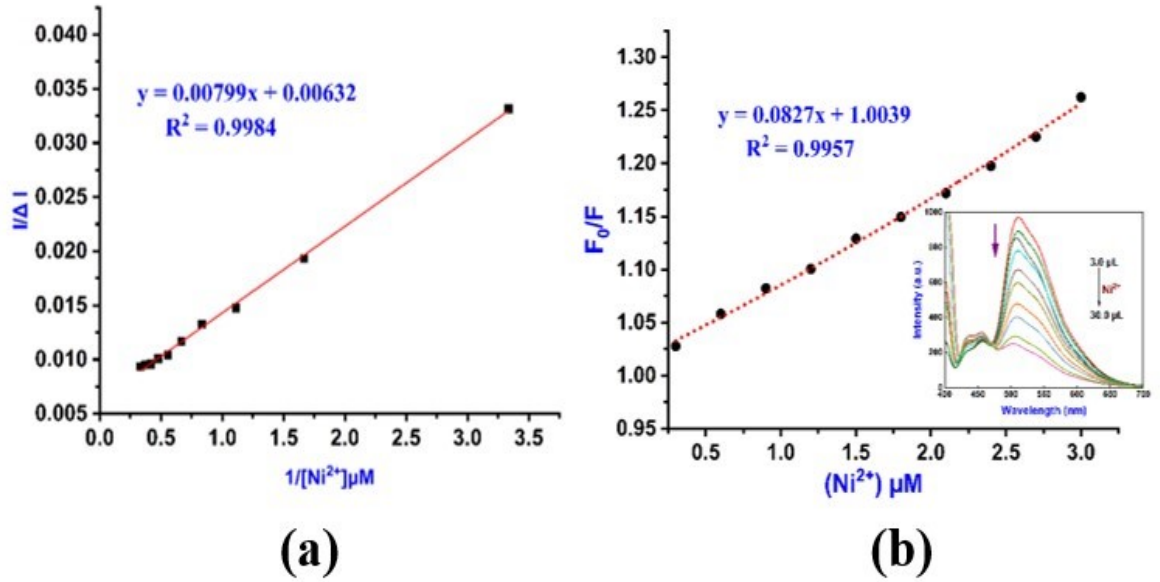

Fig. S18 (a) Association constant by B-H plot for 1:1 stoichiometry for **MG** between Ni^{2+} (3 µL-30 µL) and **HL** (10 µM, THF) (b) Stern-Volmer plot to determine fluorescence quenching of Ni^{2+} (3 µL-30 µL) with **HL** (10 µM, THF)

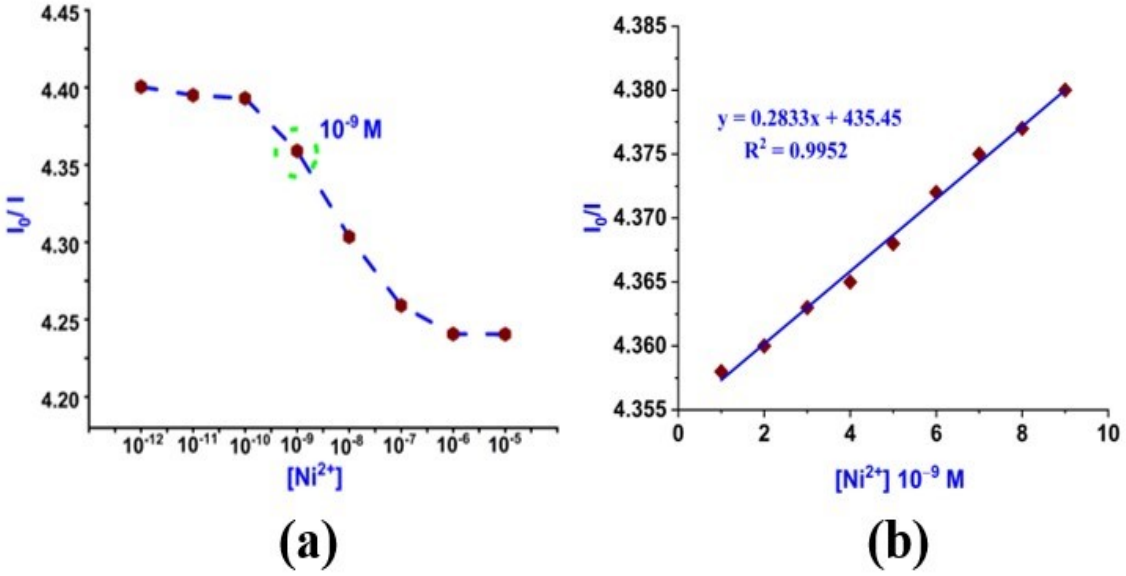

Fig. S19 (a) Sensitivity and (b) linearity plots to determine the limit of detection (LoD) interaction of Ni^{2+} with **HL** (10 μM, THF) employing the fluorescence techniques.

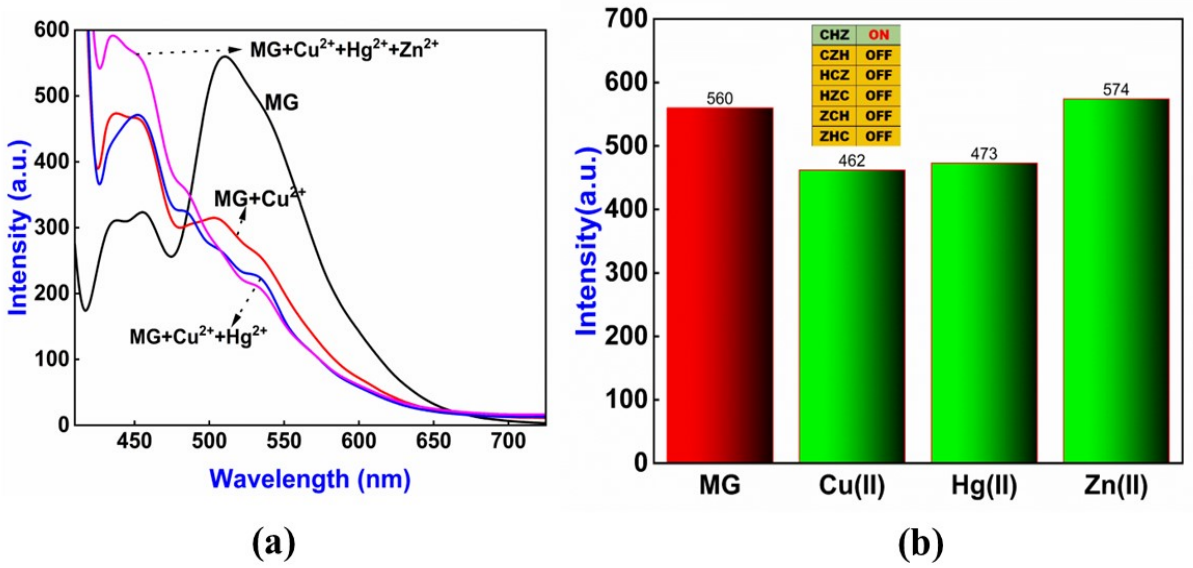

Fig. S20 Reversible emission switching behaviour of **MG** (10 μM, THF) with Cu^{2+}, $Hg^{2+}$and Zn^{2+} ions for other combinations than ZCH and ZHC (slit width 7.5 nm).

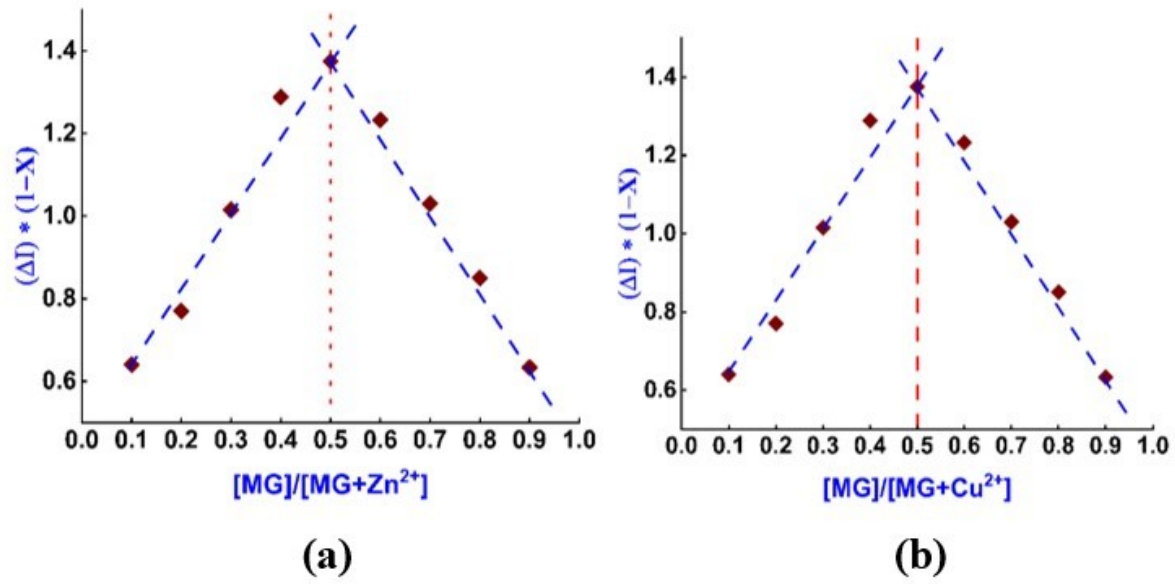

Fig. S21 Job's plot analysis showing 1:1 stoichiometric between **MG** (10 μM, THF) (a) Zn^{2+} and (b) Cu^{2+}.

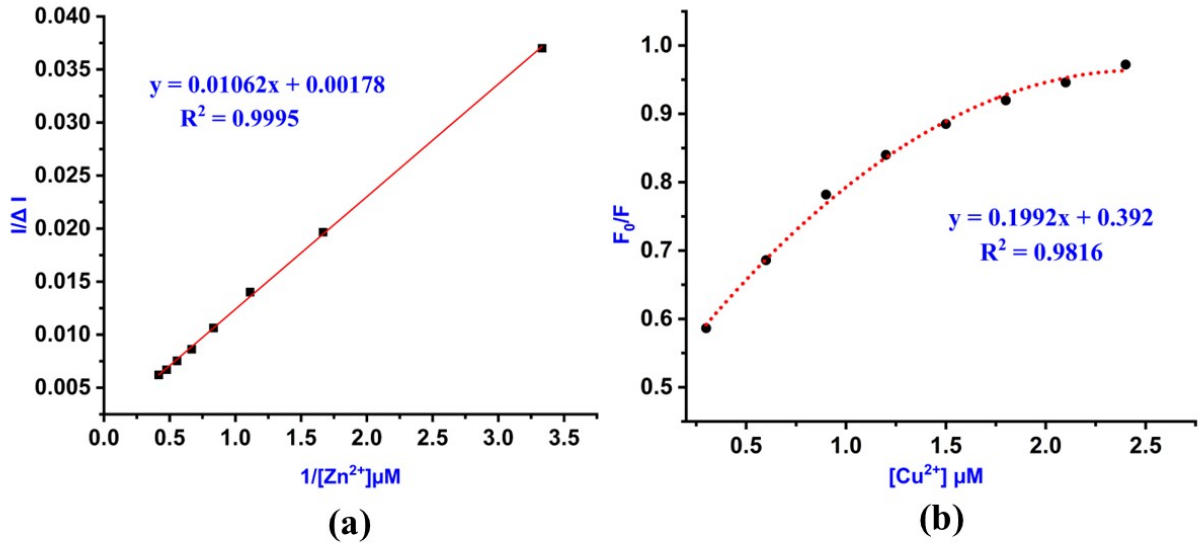

Fig. S22 (a) B-H plot for 1:1 stoichiometry for enhancement mechanism between **MG** and Zn^{2+} and (b) Stern-Volmer plot to determine fluorescence quenching of Cu^{2+} with **MG**.

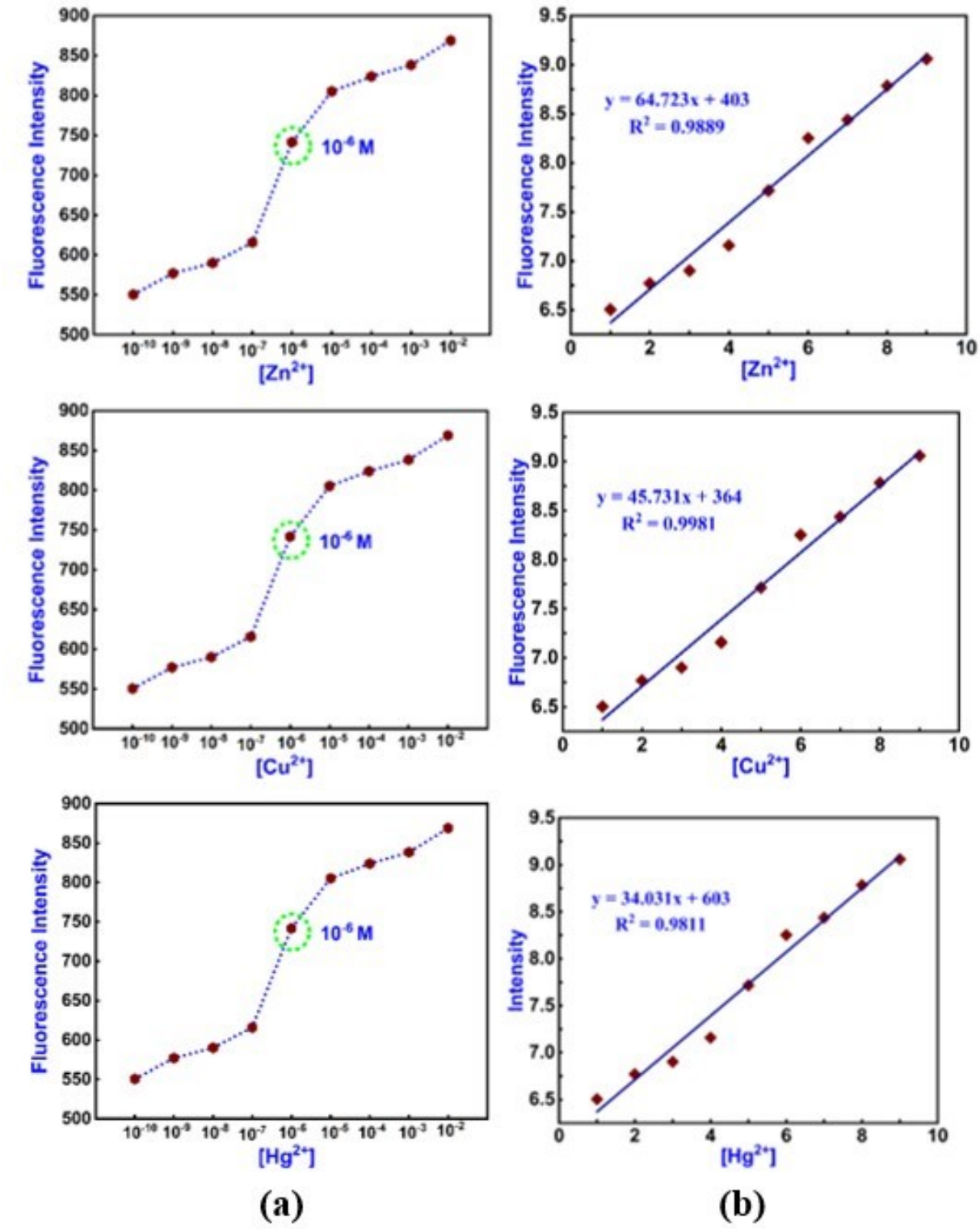

Fig. S23 (a) Sensitivity and (b) linearity plots to determine the limit of detection (LoD) interaction of detected metal ions (M^{2+}=Zn^{2+}, Cu^{2+} and Hg^{2+}) with **MG** (10 μM, THF) employing the fluorescence techniques.

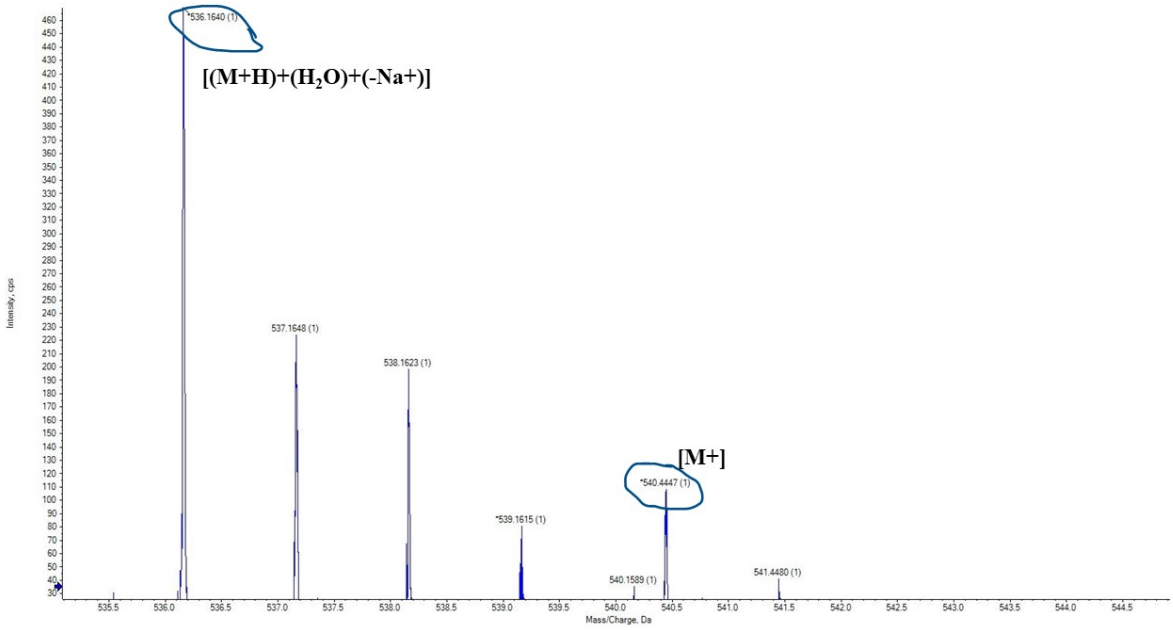

Fig. S24 HRMS spectrum of **MG**+Zn^{2+}.

The Mass spectra have been presented as below:

1. $C_{42}H_{56}N_6NiO_2$ (Complex **1**)

Experimental exact mass: 734.3803 Theoretical exact Mass: 734.3818

m/e: 734.3818 (100.0%), 735.3852 (45.4%), 736.3773 (38.5%), 737.3806 (17.5%), 736.3885 (10.1%), 738.3748 (5.3%), 738.3840 (3.9%), 739.3782 (2.4%), 735.3789 (2.2%), 737.3775 (1.7%), 737.3919 (1.5%), 740.3744 (1.4%), 736.3822 (1.0%).

(1a) Experimental Mass Spectrum of $C_{42}H_{56}N_6O_2Ni$ (Complex **1**)

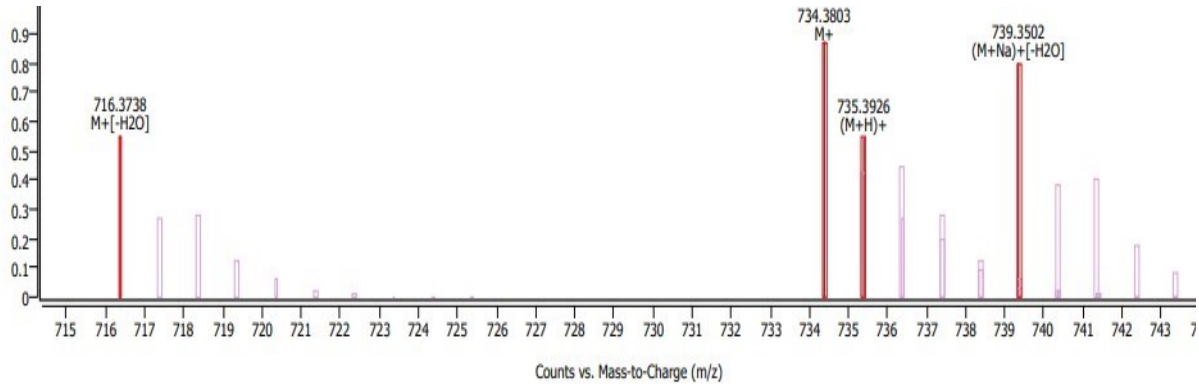

(1b) Theoretical Mass Spectrum of $C_{42}H_{56}N_6O_2Ni$ (Complex **1**) with isotopic distribution pattern

Low-resolution

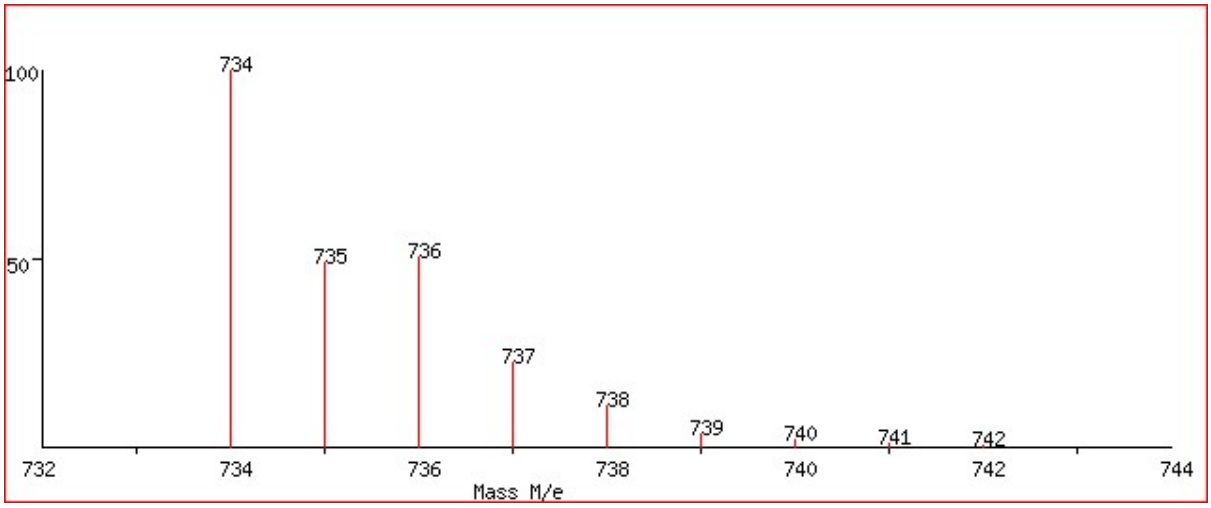

High-resolution

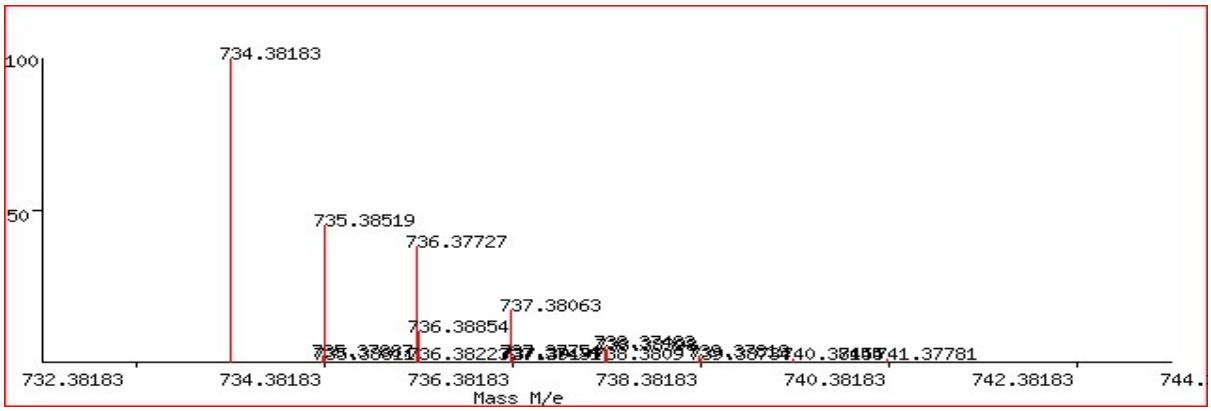

2. $C_{21}H_{30}N_4NiO_5$ (**MG**)

Experimental exact mass: 476.1590 Theoretical exact Mass: 476.157

m/e: 476.1570 (100.0%), 478.1524 (38.5%), 477.1603 (22.7%), 479.1558 (8.7%), 480.1500 (5.3%), 478.1637 (2.5%), 479.1527 (1.7%), 477.1540 (1.5%), 482.1496 (1.4%), 481.1533 (1.2%), 478.1612 (1.0%).

(2a) Experimental Mass Spectrum of $C_{21}H_{30}N_4O_5Ni$ (**MG**)

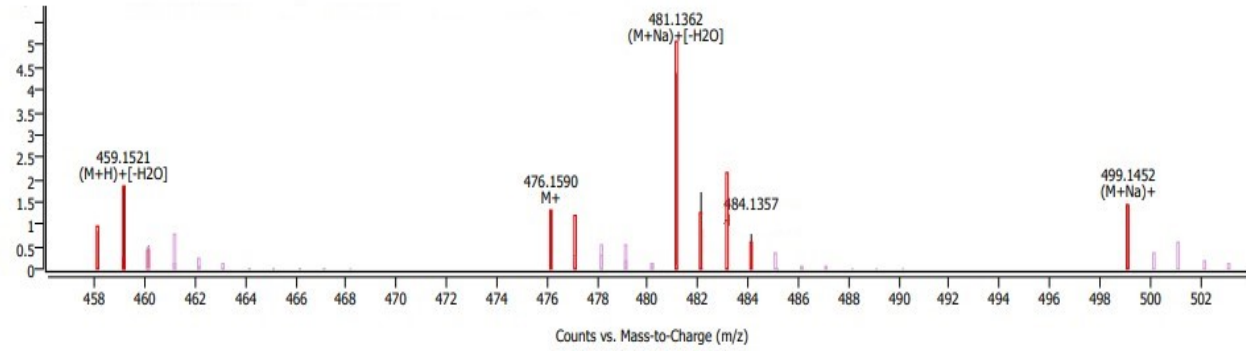

(2b) Theoretical Mass Spectrum of $C_{21}H_{30}N_4O_5Ni$ (**MG**) with isotopic distribution pattern

Low-resolution.

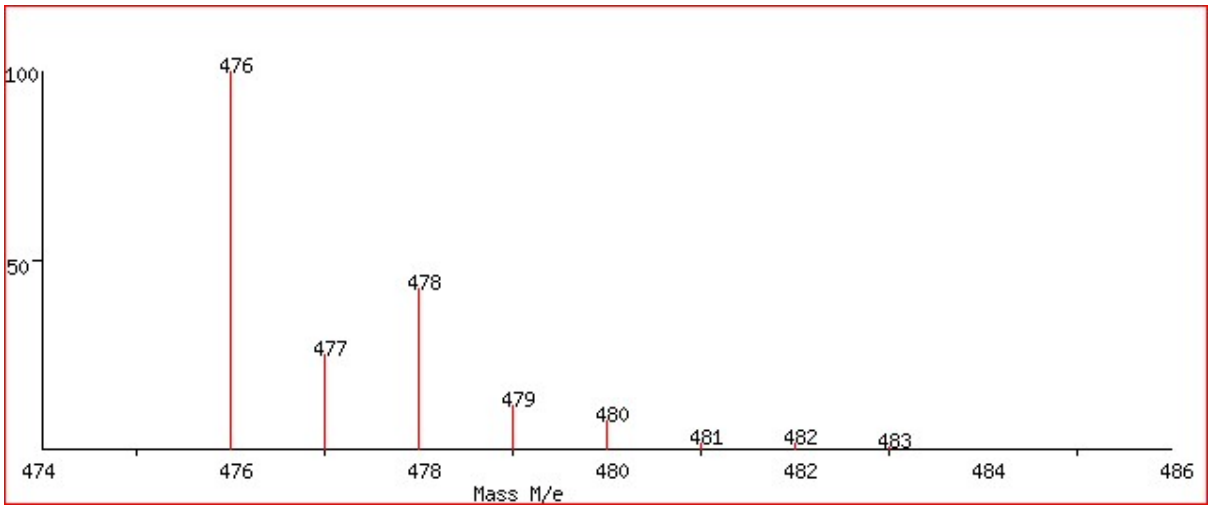

High-resolution

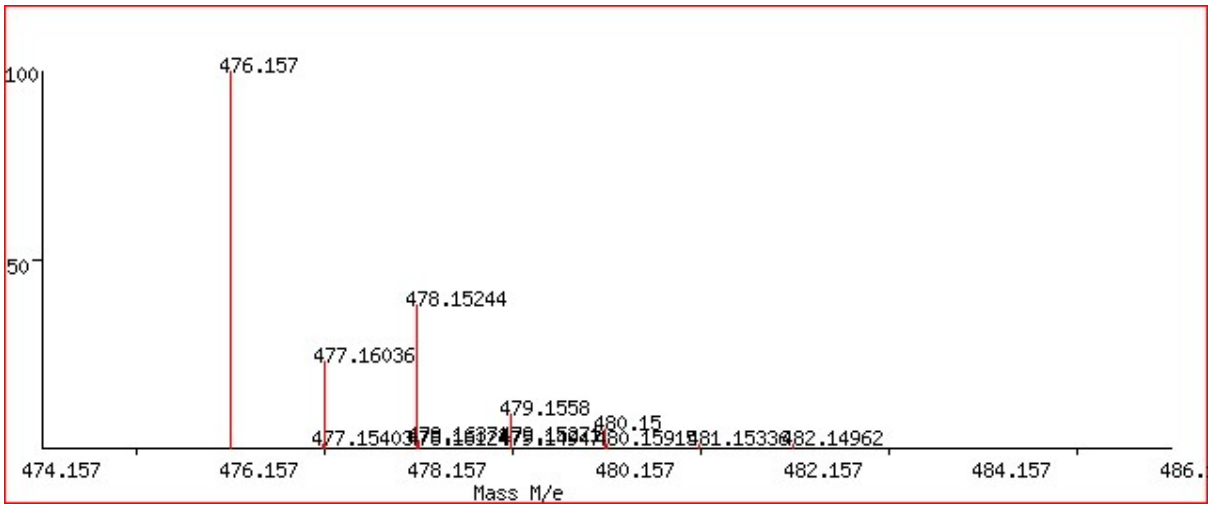

3. $C_{42}H_{56}N_6O_2Zn$ (Complex **2**)

Experimental exact mass: 741.3806 Theoretical exact mass: 740.3756

m/e: 740.3756 (100.0%), 742.3725 (57.4%), 741.3790 (45.4%), 744.3713 (38.6%), 743.3759 (26.1%), 745.3747 (17.5%), 742.3823 (10.1%), 743.3736 (8.4%), 744.3792 (5.8%), 746.3780 (3.9%), 744.3770 (3.8%), 741.3727 (2.2%), 743.3857 (1.5%), 746.3718 (1.3%), 743.3695 (1.3%), 742.3760 (1.0%).

(3a) Experimental Mass Spectrum of $C_{42}H_{56}N_6O_2Zn$ (Complex **2**)

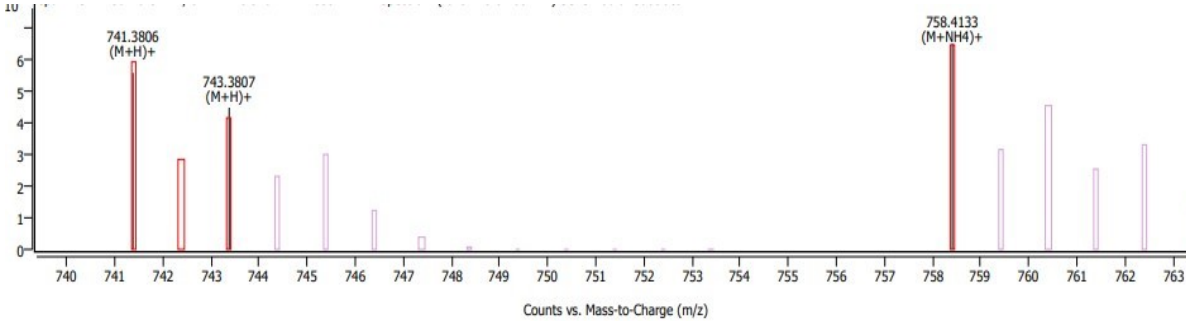

(3b) Theoretical Mass Spectrum of $C_{42}H_{56}N_6O_2Zn$ (Complex **2**) with isotopic distribution pattern

Low-resolution.

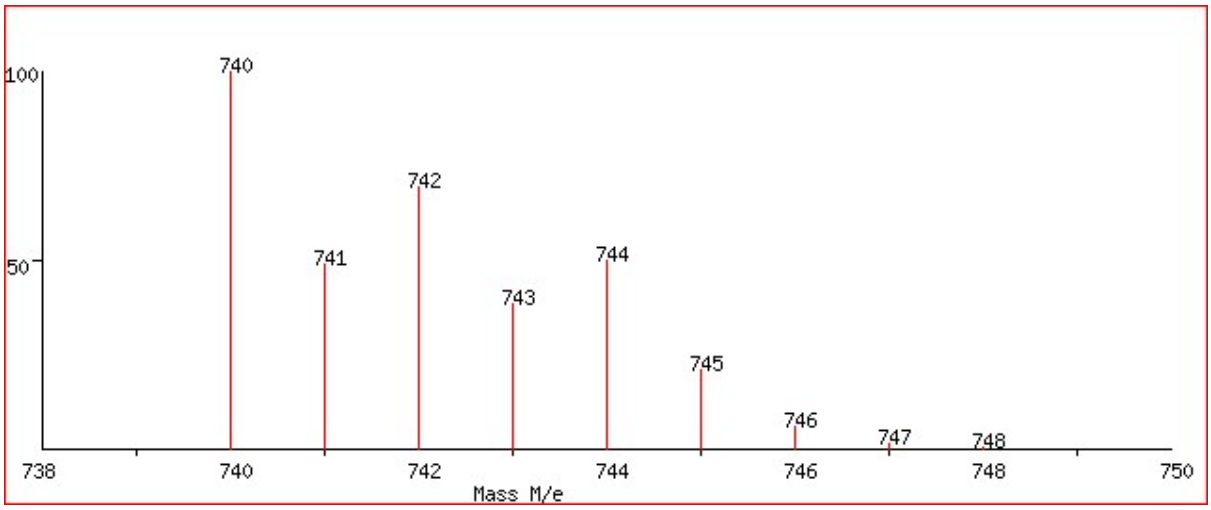

High-resolution.

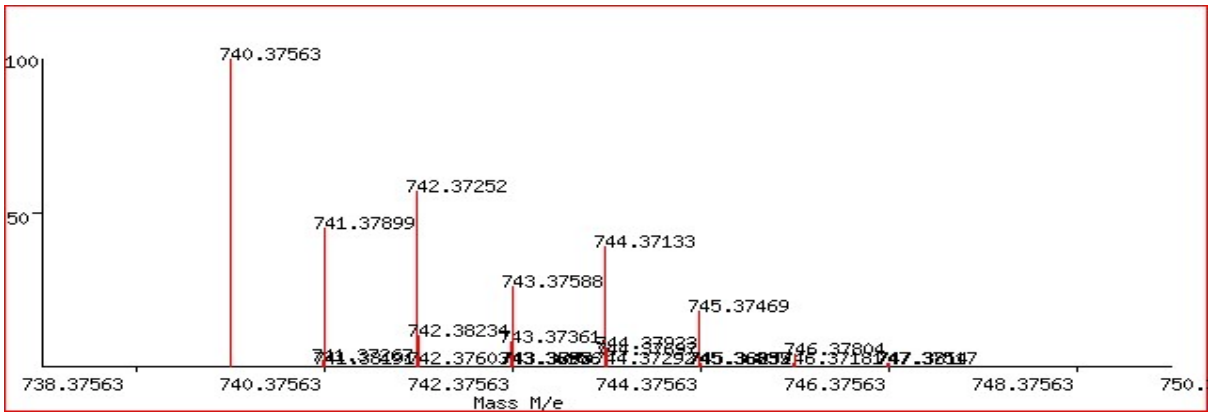

4. $C_{21}H_{30}N_4O_5NiZn$ (**MG**+Zn complex)

$C_{21}H_{30}N_4NiO_5Zn$

Experimental exact mass: 540.4447 Theoretical exact mass: 540.0861

m/e: 540.0861 (100.0%), 542.0830 (57.4%), 544.0818 (38.6%), 542.0816 (38.5%), 541.0895 (22.7%), 544.0784 (22.1%), 546.0773 (14.9%), 543.0864 (13.0%), 545.0852 (8.8%), 543.0849 (8.7%), 543.0841 (8.4%), 544.0791 (5.3%), 545.0818 (5.0%), 547.0806 (3.4%), 545.0795 (3.2%), 546.0760 (3.1%), 542.0928 (2.5%), 548.0748 (2.1%), 544.0875 (1.9%), 543.0818 (1.7%), 541.0831 (1.5%), 544.0897 (1.4%), 546.0787 (1.4%), 546.0823 (1.3%), 545.0825 (1.2%), 542.0904 (1.0%)

(4a) Experimental Mass Spectrum of $C_{21}H_{30}N_4O_5NiZn$ (**MG**+Zn complex)

(4b) Theoretical Mass Spectrum of $C_{21}H_{30}N_4O_5NiZn$ (**MG**+Zn complex) and isotopic distribution pattern

Low-resolution

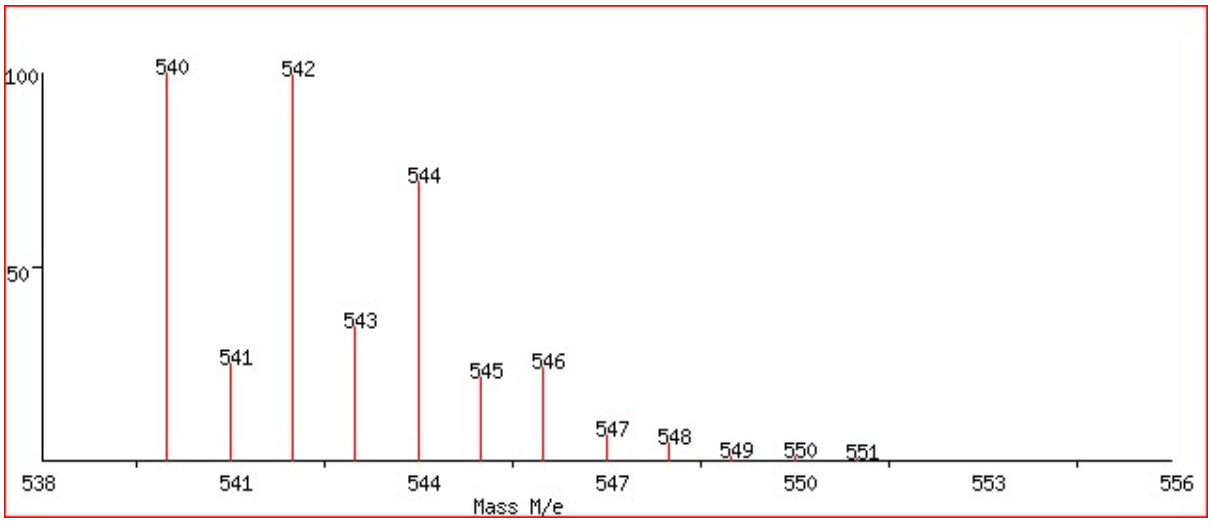

High-resolution

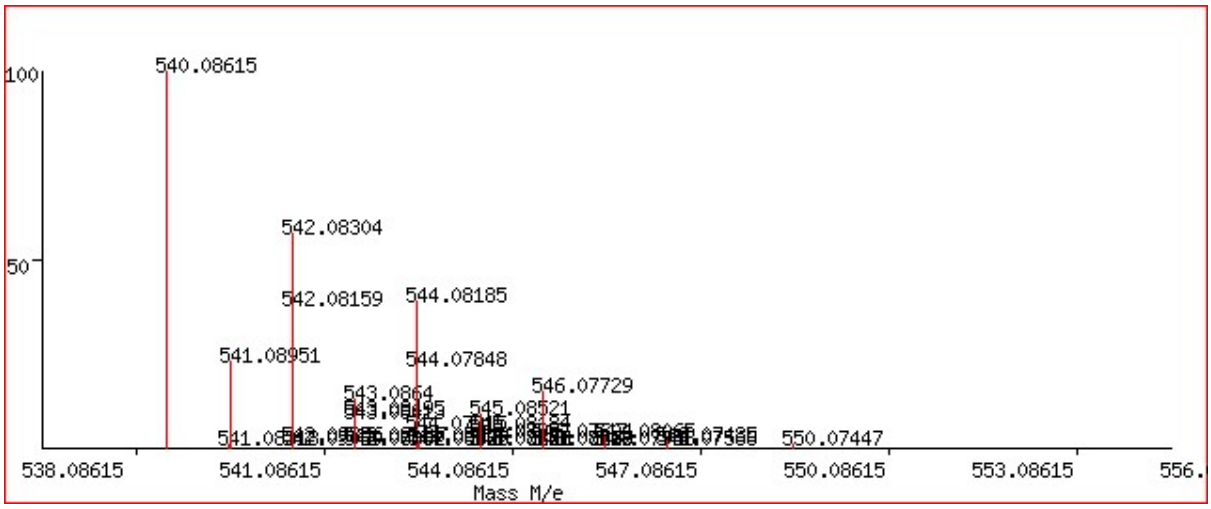

Fig. S25 Experimental and Theoretical (low-resolution and High resolution) mass spectra of the compounds.

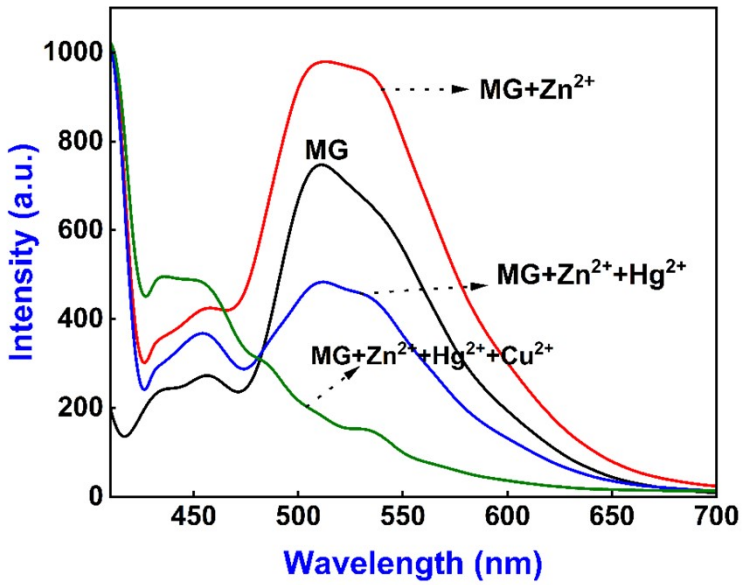

Fig. S26 Reusability experiment plots of **MG** (10 μM, THF) with Zn^{2+}, Cu^{2+} and Hg^{2+} (MeOH) after the treatment of **MG** + Zn^{2+}/Cu^{2+}/Hg^{2+} product with EDTA (1.0 equiv) (slit width 7.5 nm).